ELSEVIER

Chirp (2–7-kHz) echo characters of the South Korea Plateau, East Sea: styles of mass movement and sediment gravity flow

S.H. Lee [a,*], S.K. Chough [a], G.G. Back [b], Y.B. Kim [b]

[a] *School of Earth and Environmental Sciences, Seoul National University, Seoul 151-742, South Korea*
[b] *National Oceanographic Research Institute, Inchon 400-037, South Korea*

Abstract

The South Korea Plateau is a complex of ridges, seamount chains, troughs and a basin. Detailed analysis of 12 019 line-km Chirp (2–7-kHz) subbottom profiles from the South Korea Plateau and the eastern continental slope of Korea reveals a distinctive zonal distribution of echo types depending systematically on seafloor morphology. Pelagites/hemipelagites (type I-2) and basement highs (type III-1) prevail on the ridge summits, seamount chains and the upper to middle part of the eastern continental slope of Korea, and are commonly bounded downslope by creeps (type III-3) and slides/slumps (type IV-1) that occur extensively over the entire slope areas of the ridges, seamount chains and eastern continental slope. The mass-movement deposits change downslope to debrites and turbidites (types II, III-2, IV-2 and IV-3) in the troughs and Onnuri Basin, suggesting successive downslope evolution from slide and slump to debris flow and turbidity current. The voluminous creeps, slides and slumps over the entire slope areas of the plateau and eastern continental slope, deeper than 300 m in water depth, were most likely generated by frequent seismic shakings. © 2002 Elsevier Science B.V. All rights reserved.

Keywords: South Korea Plateau; Chirp (2–7-kHz) subbottom profiles; submarine slope failures; mass flows; submarine creep; East Sea

1. Introduction

High-frequency (3.5–12-kHz) subbottom profiling has served as an invaluable tool for the study of depositional and erosional processes in deep-sea environments (Hollister and Heezen, 1972; Damuth, 1975, 1980; Embley, 1976; Damuth and Hayes, 1977; Jacobi and Hayes, 1982, 1992; Chough et al., 1985a,b; Klaus and Ledbetter, 1988; Pratson and Laine, 1989; Dowdeswell et al., 1997; Piper et al., 1999; Wynn et al., 2000; Zaragosi et al., 2000). The types and regional distributions of reflected echoes are an important basis for the interpretation of depositional and erosional processes. The reflected echoes are mainly controlled by surface topography, subsurface geometry, and sedimentary texture of the sequence (Damuth, 1975, 1980; Embley, 1976; Damuth and Hayes, 1977). Highly variable and complex surface topography of submarine plateau

---

and ridge, however, generally causes relatively poor acoustic images and abrupt changes in the reflected echoes, hampering detailed studies on echo types and their regional distributions.

The South Korea Plateau in the western part of the East Sea is characterized by highly rugged topography (Chough et al., 2000) (Figs. 1A and 2). Recent acquisition of large amounts of densely spaced (∼5.5-km intervals) Chirp (2–7-kHz) sub-bottom profiles from the plateau (Fig. 1B) provides an unprecedented dataset for detailed analysis of echo characters in complex morphologic areas. Furthermore, the digital, wide-band frequency and matched-filter correlation processing of the Chirp profiling system generate higher-resolution (ca. 10–20-cm scale) images than those (ca. meter scale) of the 3.5-kHz system (Schock et al., 1989; LeBlanc et al., 1992). Thus, it is especially useful for delineating sedimentary processes in highly variable, complex topographic areas. The Chirp subbottom profiles in the South Korea Plateau image a variety of mass-movement and gravity-flow deposits on the entire plateau. This paper details Chirp echo characters and regional distribution of these deposits and suggests a possible triggering mechanism for extensive mass movements and slope failures.

2. Physiography

The East Sea (Sea of Japan) is a semi-enclosed back-arc basin surrounded by the eastern Asian continent and Japanese islands (Fig. 1A). In the west, the continental shelf is dominantly flat and narrow (< 20 km wide). Fluvial sediment input to the shelf has been insignificant due to the lack of large-scale rivers along the eastern coast of Korea (Chough et al., 2000). The shelf drops abruptly onto the steep (2–8°) continental slope (Fig. 2). Between 36°20′N and 37°15′N, the continental shelf and upper continental slope are characterized by the Hupo Bank and Hupo Trough that are aligned parallel to the N–S-trending shoreline (Yoon and Chough, 1995) (Fig. 2). The Hupo Bank is ∼100 km long and varies in width from < 1 to 14 km. Its top is relatively flat and lies between 100 and 200 m depth. The Hupo

Trough is ∼230 m deep at the eastern boundary and gradually shoals landward. East of the bank, the slope gradient increases to 8–10° (Fig. 2). The continental slope is devoid of large-scale, distinctive submarine canyons and channels (Yoon and Chough, 1995), and passes abruptly onto the flat basin floor of the Ulleung Basin at water depths of 2000–2100 m (Fig. 2).

To the north of 37°15′N, the continental shelf and slope trend NW–SE (Fig. 2). The shelf width reduces northward by up to 5 km. The continental slope is initially < 3°, but increases northward to 8–10°. It is characterized by a few small-scale V- or U-shaped transverse channels and gullies which are mostly restricted to the continental slope (Yoon et al., 1996) (Fig. 2). The continental slope is bounded on the east by the Korea Plateau at water depths of 1000–1500 m.

The Korea Plateau is a topographically rugged feature with 1000–1500 m of relief. It separates the Ulleung and Japan basins, the latter depression indenting the plateau divides it into the North and South components (Chough et al., 2000) (Fig. 1A). The plateau ends abruptly to the south against an E–W- to ENE–WSW-trending escarpment (Fig. 2). It is bounded on the north by the Wonsan Trough (Fig. 1A). In the east, the plateau abruptly passes into the flat basin floor of the Japan Basin in the northern part and into the Ulleung Interplain Gap connecting the Ulleung Basin to the Japan Basin in the southern part (Fig. 1A).

The South Korea Plateau consists of numerous ridges, seamount chains, and intervening troughs and Onnuri Basin trending N–S or NE–SW (Chough et al., 2000) (Fig. 2). The ridges and seamount chains occur at about 600–1500 m water depth. The ridges are relatively broad (> 30 km wide) and rarely exceed 1° in slope gradient, mostly ranging from 0.1 to 0.5° except near the ridge summits and small-scale topographic highs rising about 200–300 m above the surrounding seafloor (Fig. 2). In contrast, the seamount chains are mostly steep and narrow (< 10 km wide). The ridges and seamount chains are commonly bounded by troughs and Onnuri Basin (Fig. 2). The troughs and Onnuri Basin occur at about 1500–2200 m water depth and are 15–40
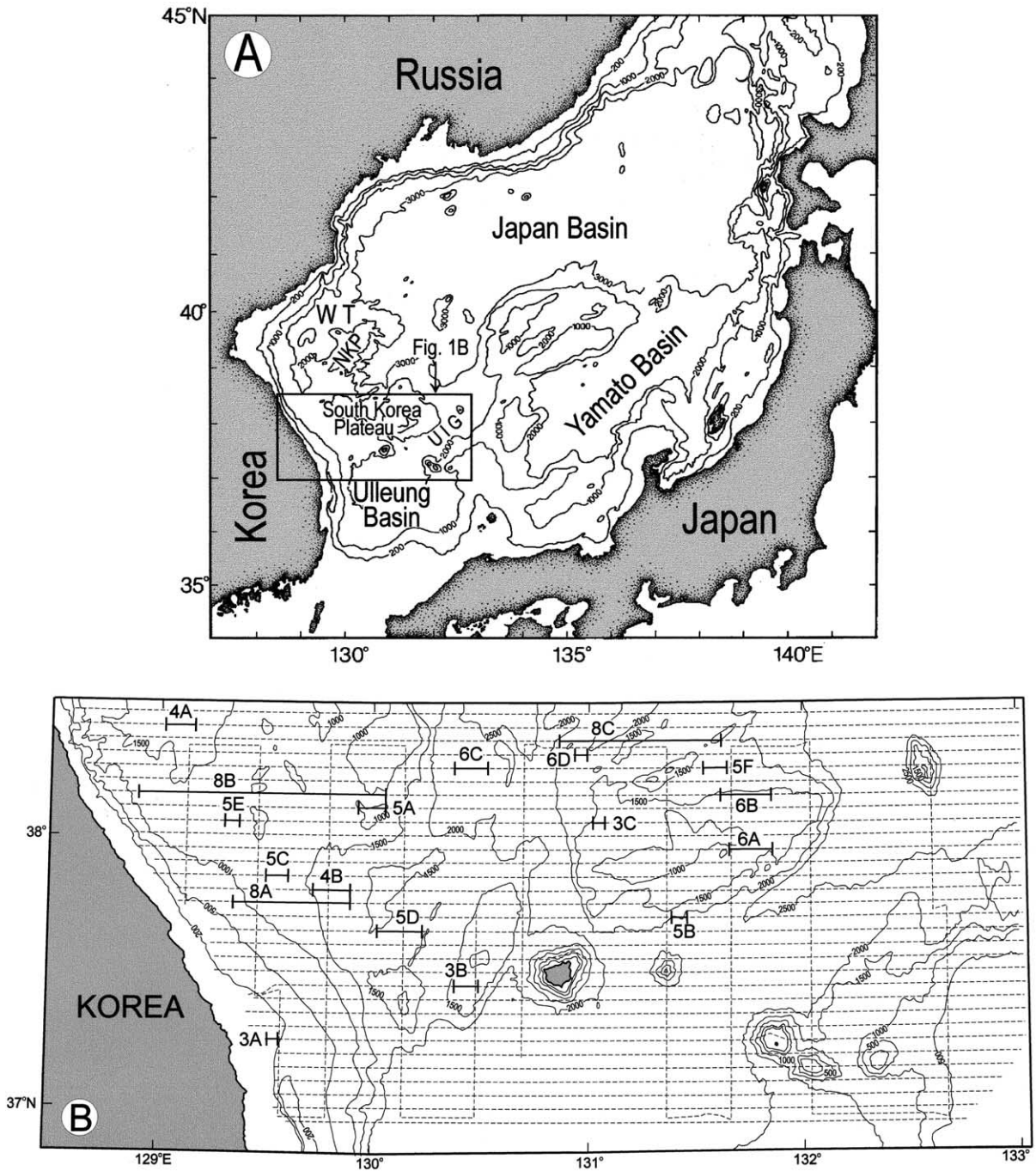
Fig. 1. (A) Major physiographic features of the East Sea (Sea of Japan). NKP = North Korea Plateau; UIG = Ulleung Interplain Gap; WT = Wonsan Trough. (B) Map showing tracklines of Chirp (2–7-kHz) subbottom profiles. E–W tracklines are spaced at approximately 5.5-km intervals. Numbers with thick bars indicate the location of Figs. 3–6 and 8. In A and B bathymetry in meters.
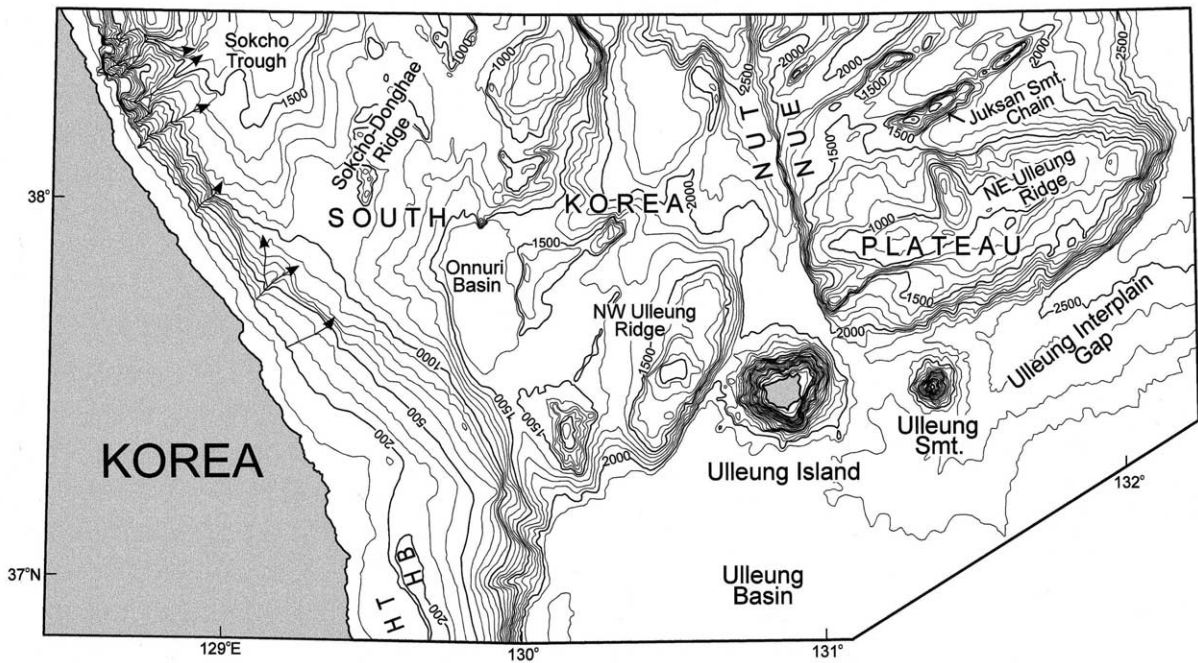
Fig. 2. Detailed bathymetry and physiographic features of the South Korea Plateau and the eastern continental slope of Korea. Bathymetry in meters. Contour interval is 100 m. HB = Hupo Bank; HT = Hupo Trough; NUE = North Ulleung Escarpment; NUT = North Ulleung Trough; Smt. = seamount. Arrows indicate small-scale transverse gullies and channels on the eastern continental slope of Korea.

km wide. The Sokcho Trough deepens northward and extends to the Japan Basin. The South Korea Plateau is divided into the western and eastern parts by the North Ulleung Trough (Fig. 2). This depression deepens northward along the North Ulleung Escarpment and extends to the Japan Basin. In the western South Korea Plateau, the ridges, troughs and Onnuri Basin dominantly trend N–S or NNE–SSW (Fig. 2). On the other hand, the eastern South Korea Plateau is characterized by ENE–WSW-trending ridges, seamount chains and troughs.
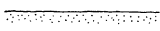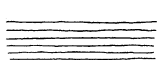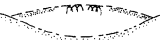
3. Data and methods
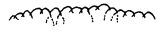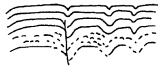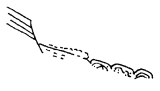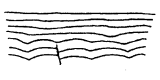
Between 1996 and 1997, the National Oceanographic Research Institute (NORI) of Korea regionally mapped the seafloor of the East Sea. During the 1997 cruise, 12 019 line-km of high-resolution subbottom profiles were collected in the area of 36°57′N–38°27′N and 128°30′E–133°00′E using a Chirp profiling system (Fig. 1B). Bathymetric data were acquired concurrently using a multi-beam echo sounder system (Sea-Beam 2100). The survey lines were mostly aligned E–W at ∼5.5-km spacings, with a few N–S survey lines. The area covered was about 58 000 km^2 (Fig. 1B). The Chirp profiling system (Data-sonics CAP-6000W), tuned-frequency profiler, emits a computer-generated FM swept pulse with a frequency band of 2–7 kHz as a source signal. Returning signals were processed using a matched-filter correlation technique in order to collect the frequency band of 2–7 kHz, which provides higher-resolution images than those of the 3.5-kHz system (Schock et al., 1989; Le-Blanc et al., 1992). Navigation was controlled using a Differential Global Positioning System (Trimble 4000RS/DS) with a positional accuracy of ± 10 m.

4. Echo types

Ten echo types are identified on the basis of

Table 1
Description and interpretation of echo types

Description and interpretation of echo types

Class	Type	Line drawing	Description	Occurrence	Interpretation
I	I-1		Very sharp surface echo with no or few diffuse subbottom reflectors; nearly flat or slightly inclined topography with slightly irregular relief; prograding geometry of diffuse internal reflections in intra-shelf topograpghic depression	Eastern continental shelf of Korea	Coarse-grained sediments on the surface (Damuth and Hayes, 1977; Pratson and Laine, 1989)
	I-2		Distinct bottom echo with several continuous internal reflectors; nearly flat to steeply inclined topography; conformable subbottom reflectors to the surface topography; 20–60 m in sound penetration depth	Summits and broad, gentle-sloping areas of the ridges and seamount chains, and the upper to middle part of the eastern continental slope of Korea	Pelagites/hemipelagites (Pratson and Laine, 1989; Yoon et al., 1996)
II	II		Acoustically transparent masses; lens-shaped or laterally wedged form; variable surface echoes ranging from seafloor-tangent hyperbolae to weak or very prolonged echoes; convex-up or nearly flat upper surface with concave-upward base	Lower part of the eastern continental slope of Korea; lower slope of the ridges and seamount chains; axis of the troughs and Onnuri Basin	Debrites (Embley, 1976; Damuth, 1980)
III	III-1		Large single or irregular overlapping hyperbolae with widely varying vertex elevations above the seafloor; strongly reflective surface echo and prolonged subbottom echoes	Ridge summits, seamount chains and escarpments; topographic highs in the eastern continental shelf and slope of Korea	Basement highs or outcrops (Damuth, 1980; Laine et al., 1986).
	III-2		Regular, intense overlapping hyperbolae with little or slightly varying vertex elevations; less than 10 m in hyperbola relief; 50–250 m in wavelength; laterally wedged geometry; convex-up upper surface and concave-upward base	Middle to lower part of the eastern continental slope of Korea; lower slope of the ridges and seamount chains; axis of the troughs	Debrites (Nardin et al., 1979; Damuth and Embley, 1981; Lee et al., 1999)
	III-3		Irregular, wavy surface echo and several continuous internal reflectors; basal mingled reflections overlying the undeformed layers; wavelength of 0.2–5 km and wave height of 2–15 m; systematic variations in both wave dimensions and thickness of internal reflectors with change in slope gradient; common internal faults in the wave troughs	Broad, gentle-sloping (<0.5°) areas of the ridges	Creep deposits (Syvitski et al., 1987; Lee and Chough, 2001)
	III-4		Wavy, prolonged bottom echo with a few indistinct, parallel subbottom echoes; 0.3–2 km in wavelength and <5 m in wave height; internal faults in wave troughs; slightly higher (5–10 m) topographic position than the adjacent echo types II and IV-1	Intervening troughs	Deformed turbidites by shearing of debris flows and slides/slumps (Damuth and Hayes, 1977; Gardner et al., 1999)
IV	IV-1		Irregular blocky, lumpy or hyperbolic masses bounded upslope by scarps or scars; highly variable degrees of internal deformation; scars marked by sharp glide plane or irregular drape of thin acoustically transparent or hyperbolic masses; several scars below the head scarp; step-like geometry of failed masses	Upper to lower slope of the ridges and seamount chains; upper to lower part of the eastern continental slope of Korea	Slide/slump deposits and mass-failure scars (Embley and Jacobi, 1977; Chough et al., 1985b)
	IV-2		Flat, distinct to indistinct surface echoes with several continuous subbottom echoes; filling geometry on the depressions; nearly flat internal reflectors in the upper part and wavy internal reflectors with a subbottomward increase of wave amplitude in the middle to lower part; small-scale internal faults in the wavy part	Axis of the troughs	Turbidites (Pratson and Laine, 1989; Chough et al., 1997); wavy internal reflectors in the middle to lower part: deformation (O'Leary and Laine, 1996)
	IV-3		Laterally wedged transparent masses and indistinct stratified masses; filling geometry in the depressions; transparent masses: convex-up to nearly flat upper surface and concave-up base, often bounded below by the eroded indistinct stratified masses; indistinct stratified masses: partly disrupted reflections	Axis of the troughs	Interlayered debrites (transparent masses) and turbidites (indistinct stratified masses) (Embley, 1976; Chough et al., 1997).
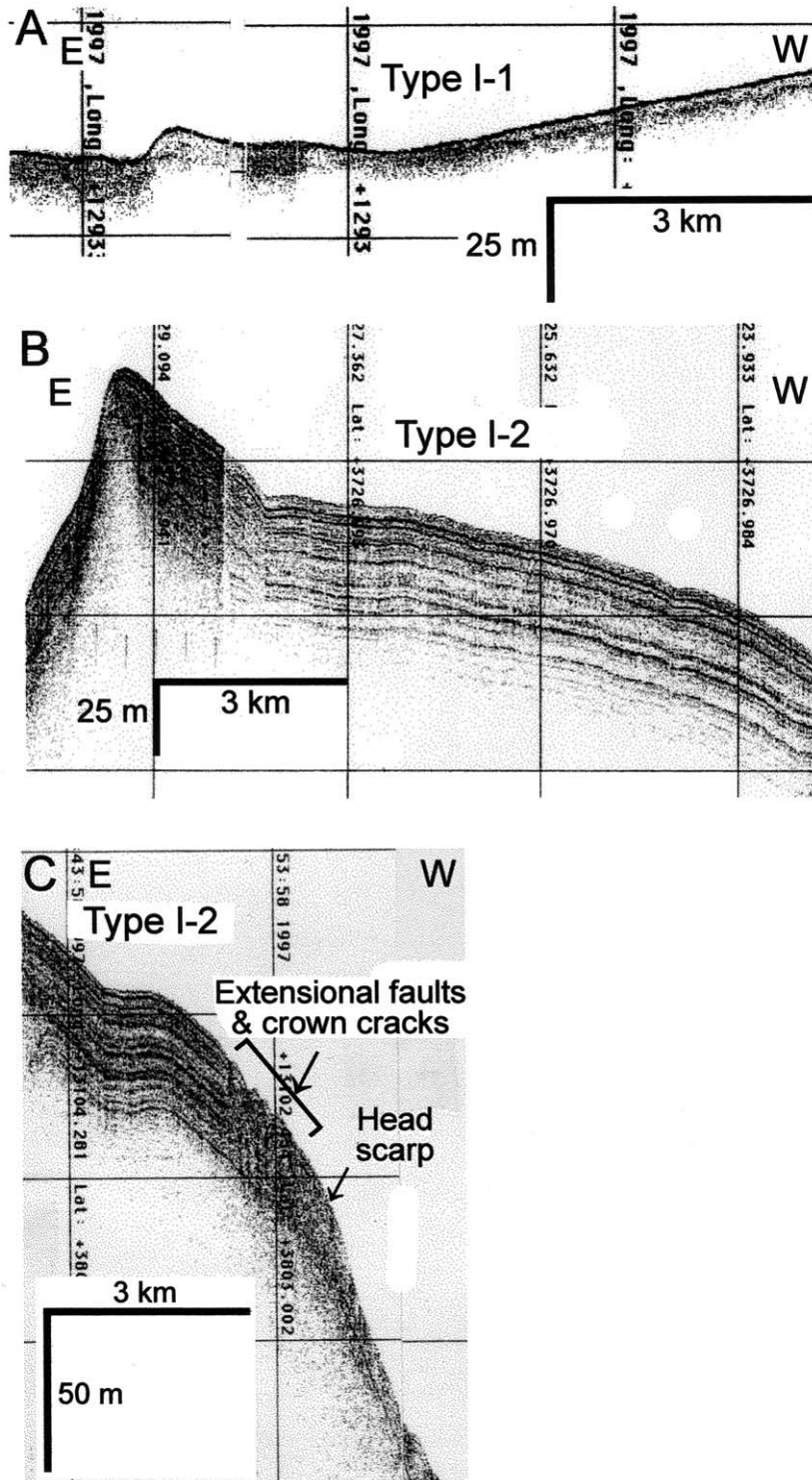
clarity, continuity, geometry of the bottom and subbottom echoes, as well as the seafloor morphology (Table 1). These types are classified into four major classes: (1) distinct echoes (types I-1 and I-2), (2) indistinct echoes (type II), (3) hyperbolic or wavy echoes (types III-1 to III-4), and (4) combined echoes (types IV-1 to IV-3) based mainly on the schemes of Damuth (1980) and Chough et al. (1985b).

4.1. Distinct echoes (I)

4.1.1. Type I-1

Type I-1 is characterized by very sharp surface reflector with no or few diffuse subbottom echoes (Fig. 3A). The surface echo shows nearly flat or gently sloping topography with slightly irregular relief. In the intra-shelf topographic depressions, diffuse internal reflectors often show prograding geometry.

The very sharp bottom echo with no or rare internal reflectors reflects dominance of coarse-grained sediments such as sands and gravels on the surface (Damuth and Hayes, 1977; Pratson and Laine, 1989).

4.1.2. Type I-2

This type consists of distinct bottom echo and several continuous, parallel internal reflectors that are conformable to the surface topography (Fig. 3B,C). The surface echo shows nearly flat to steeply inclined topography. This type ranges from 20 to 60 m in sound penetration depth. In the eastern South Korea Plateau, it is thinner than that in the western South Korea Plateau. Type I-2 is commonly dissected downslope by head scarps or scars (Fig. 3C). Above the head scarps, this type exhibits slightly wavy, diffuse internal reflectors with synthetic, extensional faults and crown cracks (Fig. 3C). The extensional faults have only small displacements in the order of a few meters and dip downslope. Type I-2 mostly occurs on the topographic highs and the

upper to middle part of the eastern continental slope of Korea. In cores, this type consists dominantly of bioturbated muds (Table 2; Yoon et al., 1996).

Although type I-2 can be interpreted as turbidites or pelagic/hemipelagic sediments, the conformity of internal reflectors with the surface topography, the occurrence on the topographic highs, and the dominant bioturbated muds in cores favor pelagic/hemipelagic origin (Pratson and Laine, 1989; Yoon et al., 1996; Chough et al., 1997). The eastward thinning of type I-2 reflects that sedimentation rate decreased to the east.

4.2. Indistinct echoes (II)

Type II represents laterally wedged, internally transparent masses (Fig. 4). Bottom echoes are highly variable, ranging from meager, weak echoes through very prolonged echoes to seafloor-tangent hyperbolae. Sediments of this type commonly fill the depressions and exhibit either solitary unit or stacked form of several units (Fig. 4). On contour-parallel section, it generally displays either convex-up or nearly flat upper surface with concave-upward base. The lower base is often bounded below by eroded sedimentary sequence (Fig. 4A, open arrow). This type consists of several-meters-thick homogeneous muds with minor occurrence of thinly laminated muds and bioturbated muds (Table 2; KORDI, 1995).

The laterally wedged geometry and the internal acoustic transparency have been recognized as the most conspicuous features of debrites (Embley, 1976; Piper et al., 1985). This transparency reflects internal homogenization, probably resulting from a disintegration of slope-failed masses by shear deformation and mixing with an ambient water during debris-flow formation (Middleton and Hampton, 1973; Nardin et al., 1979). The various bottom echoes appear to be related to bedforms developed on the surface of mass-flow deposits (Masson et al., 1998; Lee et al., 1999).

Fig. 3. Chirp subbottom profiles of distinct echoes (I). For location of each profile, see Fig. 1B. (A) Sharp surface echo with no or few diffuse internal reflectors (type I-1). (B,C) Distinct bottom echo with several continuous internal reflections (type I-2). Note crown cracks and small-scale, synthetic extensional faults above the head scarp in (C).
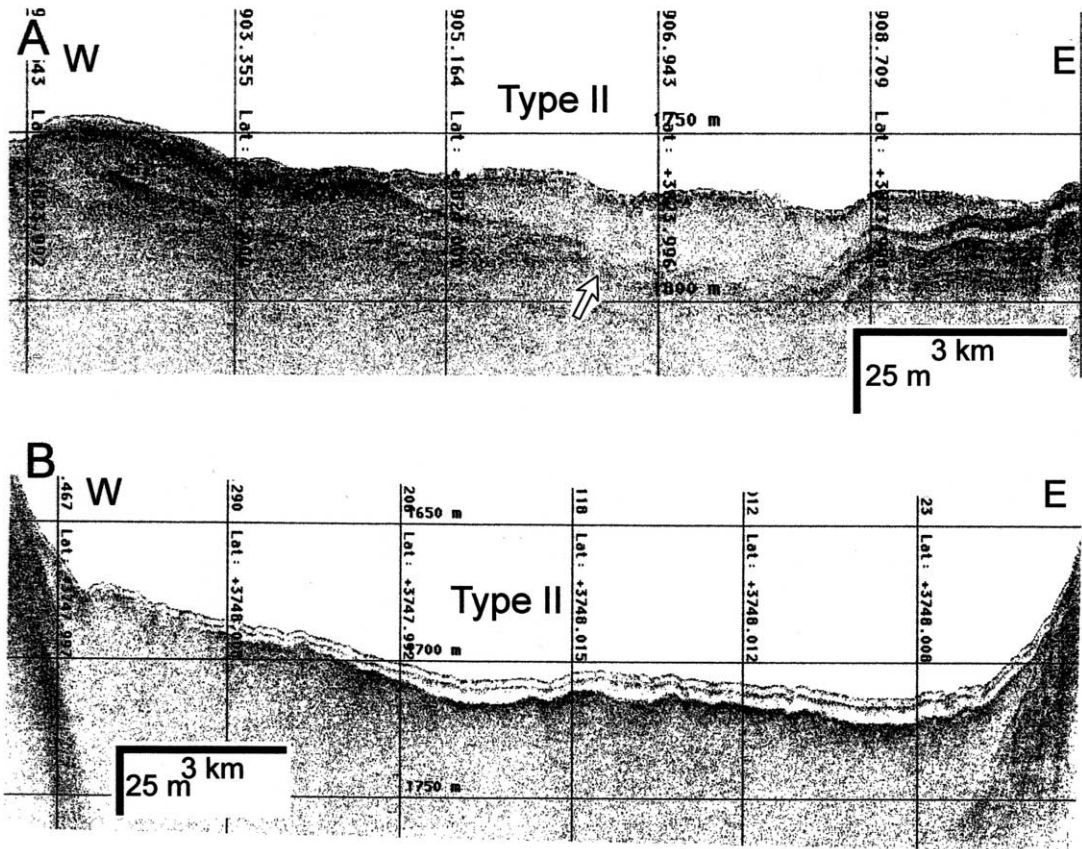
Fig. 4. Chirp subbottom profiles showing laterally wedged, acoustically transparent masses (type II). For location of each profile, see Fig. 1B. Acoustically transparent layers lying within the depressions. Note erosion into the underlying transparent layer (open arrow in A).

4.3. Hyperbolic or wavy echoes (III)

4.3.1. Type III-1

This type is characterized by large single or irregular overlapping hyperbolae with widely varying vertex elevations above the seafloor (Fig. 5A,B). Each hyperbola generally shows very strong surface echo and prolonged subbottom echoes.

The large, strongly reflective, single or irregular overlapping hyperbolae with widely varying vertex elevations above the seafloor are suggestive of basement highs or outcrops (Damuth, 1980; Laine et al., 1986; Wynn et al., 2000).

4.3.2. Type III-2

Type III-2 has regular, intense overlapping hyperbolae with little or slightly varying vertex ele-

Fig. 5. Chirp subbottom profiles showing hyperbolic or wavy echoes (III). For location of each profile, see Fig. 1B. (A,B) Large single or irregular overlapping hyperbolae with widely varying vertex elevations (type III-1). (C) Regular, intense overlapping hyperbolae with little or slightly varying vertex elevations (type III-2). Note eroded underlying stratified layers (open arrow). (D,E) Irregular, wavy surface echo and distinct to indistinct, continuous internal reflectors (type III-3). Note basal mingled or transparent reflections in D. A subbottomward increase in wave amplitude (open arrow in E). NIF = normal internal fault. CIF = compressional internal fault. (F) Wavy, prolonged bottom echo with a few indistinct, parallel internal reflectors (type III-4). Note a slightly higher topographic position of type III-4 than the adjacent type II.
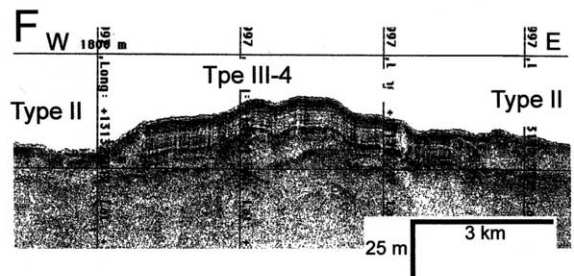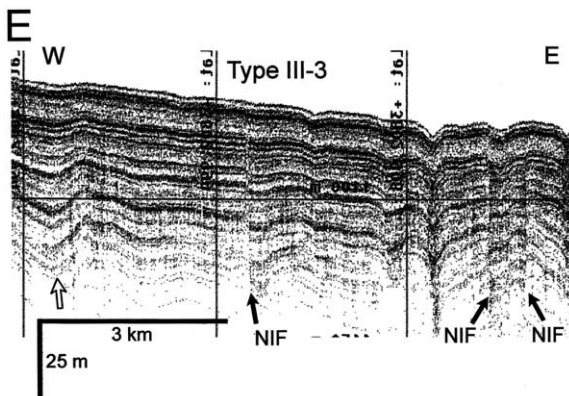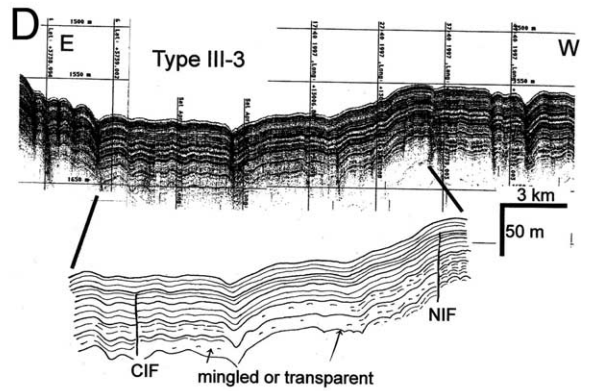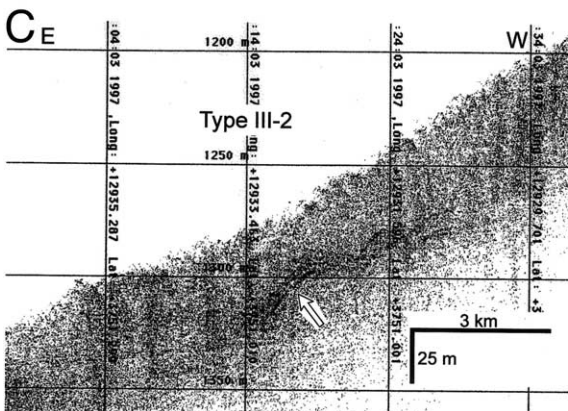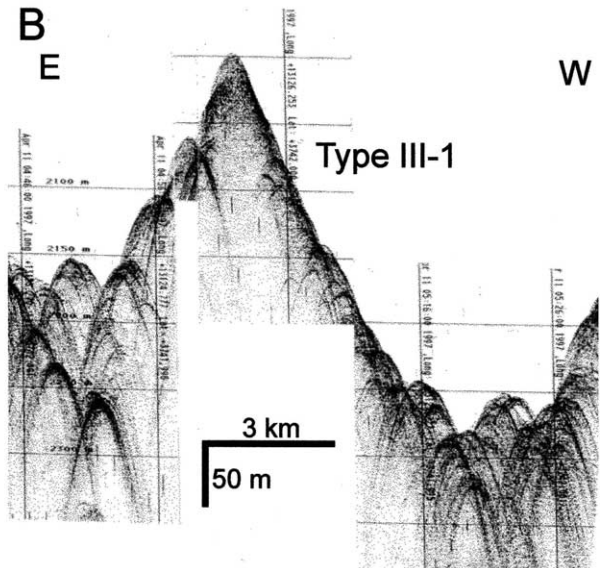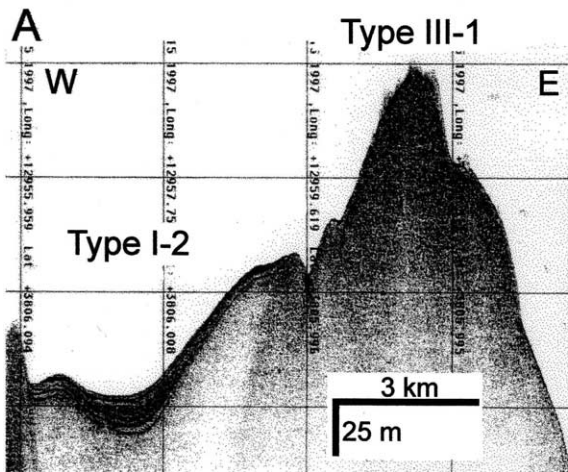
vations and no internal reflectors (Fig. 5C). Each hyperbola is generally less than 10 m in relief and 50–250 m in wavelength. Size, spacing, and elevation difference of the hyperbolae gradually decrease downslope, transforming to a very tiny hummocky terrain (Fig. 5C). This type generally exhibits laterally wedged geometry. On contour-parallel section, it commonly has convex-upward upper surface and concave-up base. Type III-2 is often bounded below by eroded sedimentary layers (Fig. 5C, open arrow). This type is commonly bounded upslope by type IV-1. In cores, type III-2 consists dominantly of mud-clast muds with minor occurrence of thinly laminated muds and bioturbated muds (Table 2; Yoon et al., 1996).

The laterally wedged geometry with regular, intense overlapping hyperbolae, the abundant mud-clast muds, and the common association with upslope slides and slumps (type IV-1) are suggestive of debrites (Damuth and Embley, 1981; Lee et al., 1999). The hummocky echoes have been commonly ascribed to bedforms on the surface of gravity-induced mass flow deposits (Normark and Gutmacher, 1988; Masson et al., 1998).

4.3.3. Type III-3

This type shows irregular, wavy surface echo and distinct to indistinct, continuous internal reflectors (Fig. 5D,E). The wavy topography exhibits a succession of broad crests and narrow troughs (Fig. 5D). Waves are 0.2–5 km long and 2–15 m high. Wave dimensions and thickness of internal reflective layers vary systematically with change in slope gradient (Lee and Chough, 2001). On relatively steep slopes, the wave displays broad spacing (1.5–5 km) and low relief (2–5 m). On the other hand, it has narrow spacing (0.2–1.75 km) with high relief (4–15 m) in the toe region downslope. Internal reflective layers are thin on relatively steep slopes and thick at the base of the slope. In the basal part, this type exhibits mingled reflections (Fig. 5D) that are correlated with chaotic reflectors overlying the undeformed sedimentary layers (Lee and Chough, 2001). Wave amplitude commonly increases with subbottom depth (Fig. 5E). Wave troughs are commonly associated with normal or compressional internal faults showing small-scale displacement (Fig. 5D,E). Type III-3 is commonly bounded downslope by type IV-1 with head scarps and scars on steeper slopes. Above the head scarps, internal faults are commonly present. This type consists dominantly of bioturbated muds with rare thinly laminated muds (Table 2; KORDI, 1995).

The basal mingled reflections overlying the undeformed layers are typical acoustic characters of internally deformed layer (Hill et al., 1982;

Table 2
Sedimentary features of echo types in cores (ca. 6–9 m long) (KORDI, 1995; Yoon et al., 1996)

Type	Major facies	Minor facies	Cores
I-2	Bioturbated muds (pelagic/hemipelagic settling)		PC-1
II	Homogeneous muds (> 5 m thick; debris flows)	Thinly laminated muds (a few centimeters thick; turbidity currents); bioturbated muds (a few centimeters thick; pelagic/hemipelagic settling)	PC-4
III-2	Mud-clast muds (1–2 m thick; debris flows)	Thinly laminated muds (a few centimeters thick; turbidity currents); bioturbated muds (a few centimeters thick; pelagic/hemipelagic settling)	PC-5, PC-9
III-3	Bioturbated muds (pelagic/hemipelagic settling)	Thinly laminated muds (a few centimeters, turbidity currents)	PC-2
IV-1	Deformed muds (1–2 m thick; slides/slumps); mud-clast muds (< 1 m thick; debris flows)	Thinly laminated muds (a few centimeters thick; turbidity currents); homogeneous muds (a few centimeters thick, turbidity currents); bioturbated muds (a few centimeters thick; pelagic/hemipelagic settling)	PC-8

For location of cores, see Fig. 7.

O'Leary and Laine, 1996). The irregular wavy, continuous reflective layers with internal faults overlying the deformed layer suggest that the wavy geometry most likely formed by deformation (Hill et al., 1982; Syvitski et al., 1987). Wave dimensions and thickness of internal reflective layers vary systematically with change in slope gradient, indicating a gravity-influenced deformation (Lee and Chough, 2001). The gravity-induced deformational structures, the common association with downslope type IV-1 (slides/slumps) on steeper slopes, and the dominant bioturbated muds suggest that type III-3 was most likely generated by creep movements of pelagites/hemipelagites (type I-2) at much smaller strains than those forming slides and slumps (Lee and Chough, 2001).

4.3.4. Type III-4

Type III-4 is characterized by irregular wavy, prolonged bottom echo with indistinct to semi-distinct, parallel subbottom reflections (Fig. 5F). Waves are 0.3–2 km long and < 5 m high. The internal reflectors are slightly disrupted (Fig. 5F). In the wave troughs, small-displaced internal faults are commonly present. This type is generally underlain and surrounded by types II and IV-1 (Fig. 5F). On contour-parallel section, it commonly occurs in slightly higher (5–10 m) topographic area than the adjacent seafloor (Fig. 5F).

The prolonged bottom echo and indistinct, disrupted internal reflections with wave geometry are suggestive of deformed turbidites (Damuth, 1980; Hill et al., 1982; O'Leary and Laine, 1996). The lateral surrounding of types II (debrites) and IV (slides and slumps) reflects that the deformation was generated by lateral shearing of debris flows, slides, and slumps (Gardner et al., 1999).

4.4. Combined echoes (IV)

4.4.1. Type IV-1

Type IV-1 comprises irregular blocky, lumpy or hyperbolic masses bounded upslope by scarps or scars (Fig. 6A,B). Below the head scarp, several scarps commonly occur (Fig. 6A). Above the head scarp, types I-2, I-3 and III-2 commonly display crown cracks and small-scale, synthetic extensional faults (Fig. 3C,E). Head regions of the scars are marked either by glide and slide planes underlain by undisturbed to slightly disturbed sediments or by irregular drapes of small-scale, thin blocky or hyperbolic or transparent masses (Fig. 6A,B). The displaced masses exhibit various degrees of internal deformation ranging from intact masses through folded or faulted internal reflectors to mingled or no internal echoes. This type often includes the slightly translated or rotated blocks of type III-3 (Lee and Chough, 2001). The scarps with displaced masses generally exhibit step-like geometry (Fig. 6A). Type IV-1 consists dominantly of deformed muds (1–2 m thick) and mud-clast muds (< 1 m thick) (Table 2; Yoon et al., 1996).

The scars and scarps, the blocky, lumpy or hyperbolic morphology of the displaced masses with deformed or transparent internal reflectors, and the dominant deformed muds are typical characters of slides and slumps (Embley and Jacobi, 1977; Chough et al., 1985b; Mulder and Cochonat, 1996).

4.4.2. Type IV-2

This type consists of flat, distinct to indistinct surface echoes and continuous subbottom reflections that are initially flat but become wavy with subbottom depth (Fig. 6C). It generally shows filling geometry in the depressions. The waveforms are irregular-spaced, and range in height from 3 to 10 m with a subbottomward increase. Small-scale internal faults occur in the wavy internal reflectors (Fig. 6C, open arrows). Type IV-2 is mainly recorded from the axis of the narrow intervening troughs. It is commonly associated upslope with types II and IV-1 (Fig. 6C).

The distinct to indistinct bottom echoes and continuous internal reflectors, the filling geometry in the depressions and the common association with upslope debrites, slides and slumps (types II and IV-1) are all suggestive of turbidites (Pratson and Laine, 1989; Chough et al., 1997). The irregular spacing and wavy internal reflectors with small-scale internal faults are typical acoustic characters of deformation (O'Leary and Laine, 1996; Gardner et al., 1999). The flat topography of surface echo and upper internal reflectors is
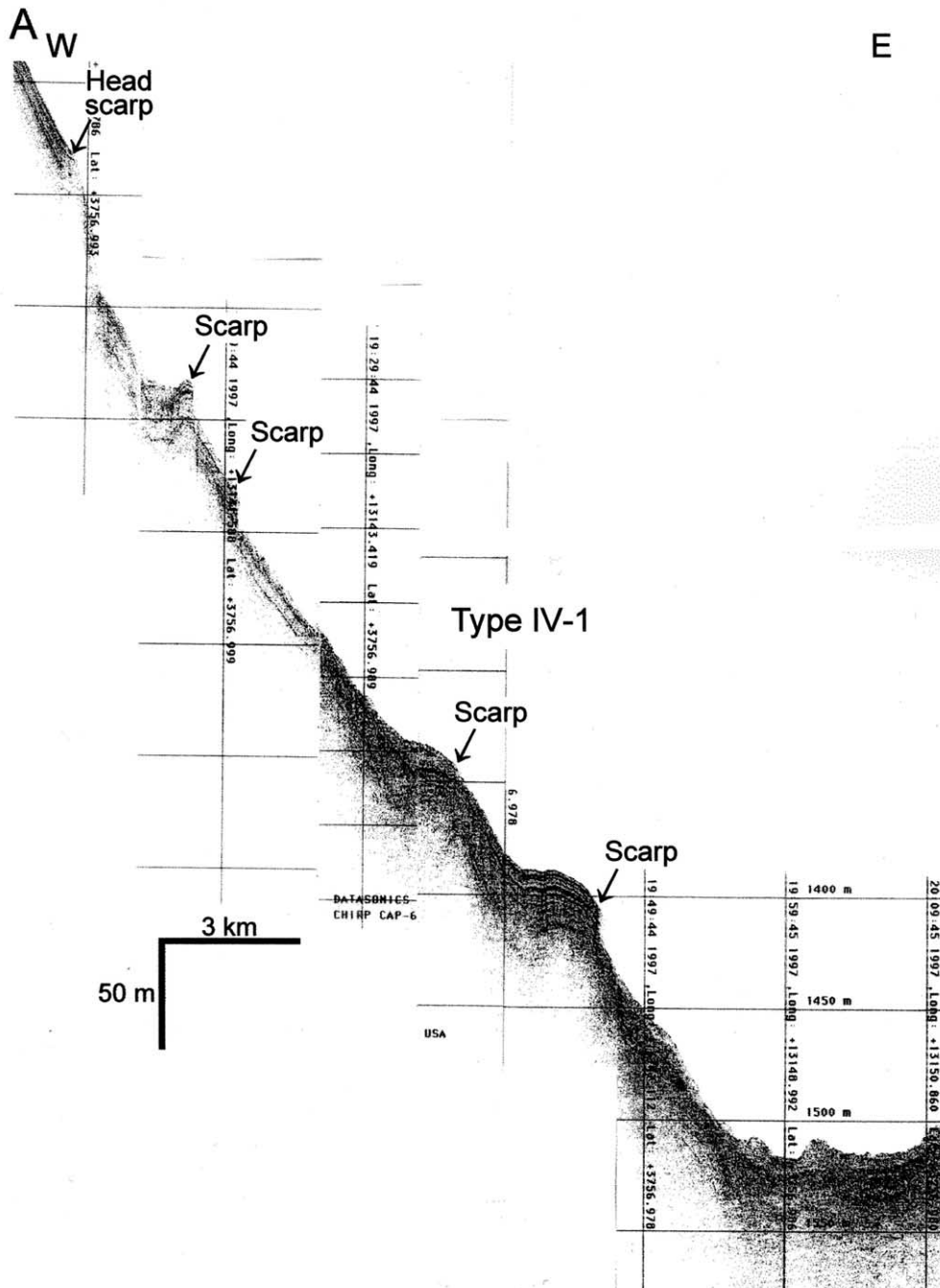
Fig. 6. Chirp subbottom profiles of combined echoes (IV). For location of each profile, see Fig. 1B. (A,B) Irregular blocky, lumpy or hyperbolic masses bounded upslope by scarps and scars (type IV-1) in contour-transverse (A) and contour-parallel (B) sections. Note several scarps below the head scarp in A. (C) Flat, distinct to indistinct surface echo with several continuous internal reflectors (type IV-2). Wavy internal reflectors in the middle to lower part with a subbottomward increase in wave amplitude. Note internal faults (open arrows). (D) Combined laterally wedged transparent masses and indistinct stratified sediments (type IV-3).

Fig. 6 (*Continued*).

suggestive of subsequent filling of turbidites upon the lower deformed, wavy subbottom reflections (Flood, 1980).

4.4.3. Type IV-3

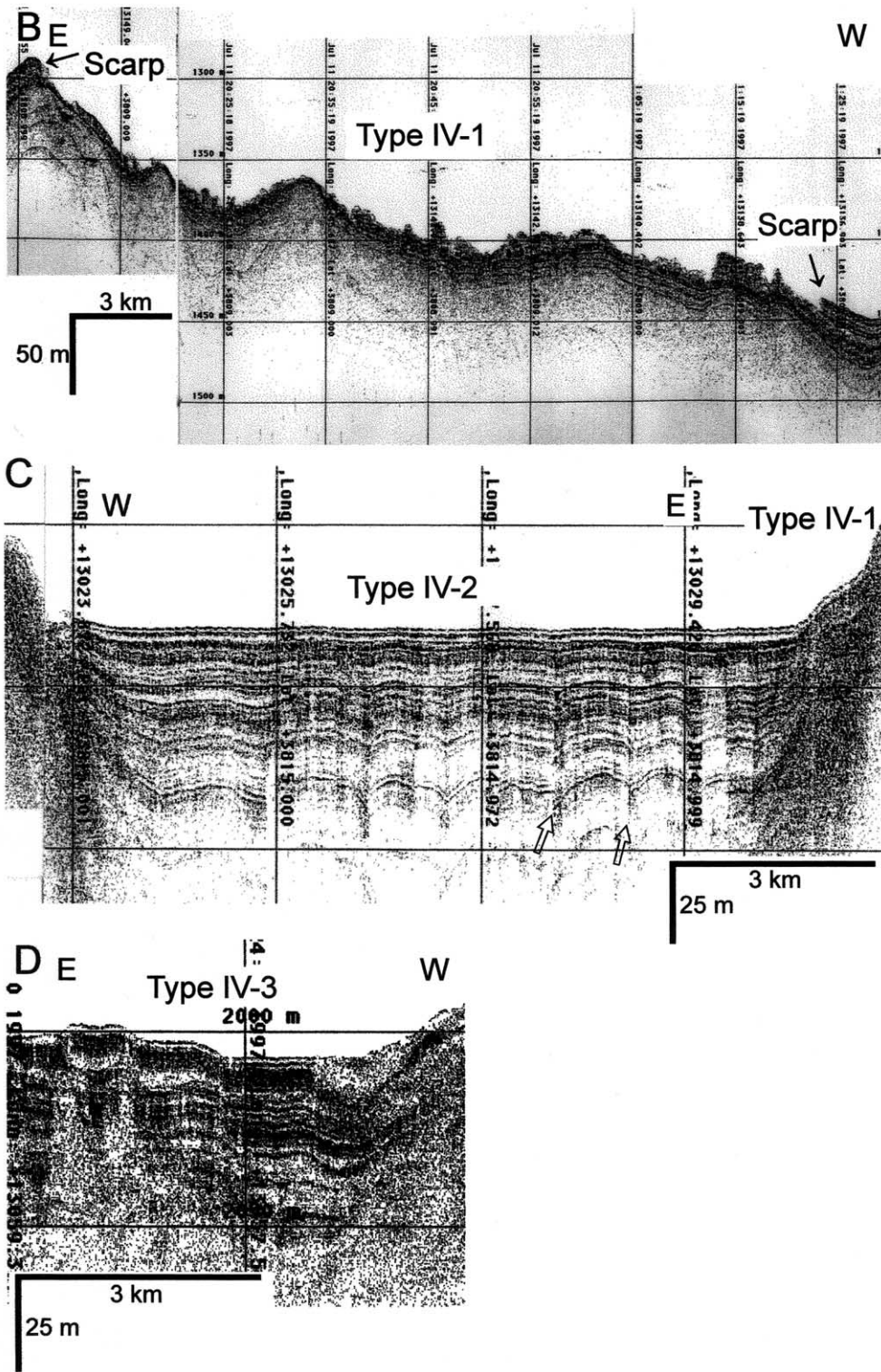Type IV-3 comprises laterally wedged transparent masses and indistinct stratified masses which commonly fill the depressions (Fig. 6D). The transparent masses generally exhibit convex-up to nearly flat upper surface and concave-up base (Fig. 6D). These masses are often bounded below by eroded indistinct stratified masses, and are less frequent in the distal part. The indistinct stratified masses often display disrupted reflectors (Fig. 6D).

Type IV-3 represents interlayered debrites (transparent masses) and turbidites (indistinct stratified masses) (Embley, 1976; Chough et al., 1997). The disrupted reflectors in indistinct stratified masses are suggestive of deformation after the deposition (O'Leary and Laine, 1996).

5. Occurrence

5.1. Eastern continental shelf of Korea

The shelf south of 37°30′N is generally dominated by types I-1 (surficial coarse sediments) and III-1 (basement highs or outcrops) (Fig. 7): the Hupo Bank and small-scale topographic highs by echo type III-1, the inner shelf and the Hupo Trough by echo type I-1.

5.2. Eastern continental slope of Korea

The continental slope region is characterized by types IV-1 (slides and slumps with scars) and I-2 (pelagites/hemipelagites) (Figs. 7 and 8A). Between 36°57′N and 37°45′N, type I-2 is dominant on the upper to middle slope, often extending to the lower slope, whereas it rarely occurs in the area between 37°45′N and 38°27′N (Fig. 7). Type I-2 is commonly truncated downslope by scarps, scars, and small-scale, transverse gullies and channels on the upper to middle slope (Fig. 8A). Large-scale blocky, lumpy or hyperbolic masses (type IV-1) are dominant downslope of the head scarps and scars. On the middle to lower slope, the displaced

slide and slump masses (type IV-1) are transitional downslope to types II and III-2 (debrites) (Figs. 7 and 8A). On the lower continental slope bounded by the Sokcho Trough and Onnuri Basin, types II and III-2 are commonly dissected by scarps and remoulded downslope into blocky, lumpy or hyperbolic masses (type IV-1), forming a step-like geometry (Fig. 8A).

5.3. Ridges (Sokcho-Donghae, NE Ulleung and NW Ulleung ridges)

The ridge summits are dominated by type III-1 (basement highs or outcrops) (Fig. 2B). The relatively flat areas of the ridge summits consist of type I-2 (pelagites/hemipelagites) with minor occurrence of type III-3 (creep deposits) (Figs. 7 and 8B). Types I-2 and III-3 are commonly truncated by scarps and scars at the upper to middle slope of the ridge summits and remoulded downslope into slide and slump masses (type IV-1) (Fig. 6A,B). Where the slopes of the ridge summits are directly bounded by the troughs (e.g., the eastern slope of the Sokcho-Donghae Ridge and the northern slope of the NE Ulleung Ridge), slides and slumps (type IV-1) generally extend to the middle to lower slope and often change to debrites (type II) on the lower slope (Fig. 7). The escarpments flanking the summits of the NE and NW Ulleung ridges are dominated by basement outcrops (type III-1) with small-scale, thin slides and slumps (type IV-1) (Fig. 7). The broad, gently sloping areas downslope of the ridge summits consist dominantly of creep deposits (type III-3) with rare occurrence of pelagites/hemipelagites (type I-2) (Figs. 7 and 8B). Types I-2 and III-3 are generally transitional downslope to slides and slumps with scars (type IV-1) on the upper to middle slopes of the ridges. The displaced slump and slide masses (type IV-1) downslope of the head scarps are commonly redissected by scarps and remoulded downslope into blocky, lumpy or hyperbolic masses, forming a step-like geometry (Fig. 6A).

5.4. Seamount chains (Juksan and other seamount chains)

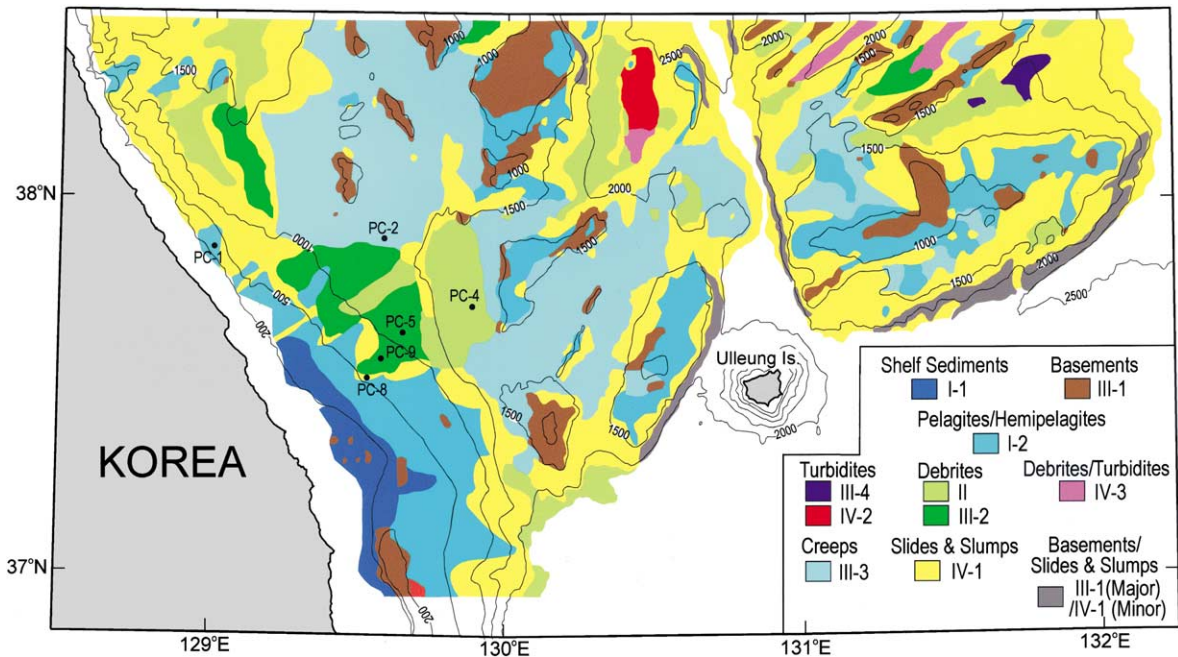The seamount chains consist dominantly of

Fig. 7. Distribution of echo types in the South Korea Plateau and the eastern continental slope of Korea.

type III-1 (basement highs or outcrops) with rare occurrence of type I-2 (pelagites/hemipelagites) (Figs. 7 and 8C). On the middle to lower slope of the seamount chains, slide and slump masses (type IV-1) generally occur without distinct scarps and scars. The slide and slump masses on the seamount chains are generally smaller than those on the ridges (Figs. 6A,B and 8C).

5.5. Intervening troughs (Sokcho and other intervening troughs)

Along the axis of the troughs, types II, III-2, IV-2, and IV-3 (debrites and turbidites) are predominant (Figs. 7 and 8B,C). These debrites and turbidites are generally associated upslope with type IV-1 (slides and slumps with slope failures) on the slopes of ridges and seamount chains and the eastern continental slope of Korea. In the Sokcho Trough and the trough north of the NE Ulleung Ridge, bounded by the relatively wide, gentle slopes of the ridges and the eastern continental slope, types II and III-2 (debrites) are dominant (Figs. 7 and 8B). On the other hand, the

intervening troughs bordered by the narrow, steep slopes of the seamount chains and ridges consist dominantly of types IV-2 and IV-3 (turbidites) with minor occurrence of debrites (types II and III-2) (Figs. 7 and 8B). The occurrence of debrites (types II, III-2 and transparent masses in type IV-3) diminishes toward the distal area.

5.6. Onnuri Basin

The entire floor of the Onnuri Basin is dominated by debrites (type II) (Figs. 7 and 8A). The large areas of slope failure and related mass movement (types IV-1, III-2, and II) on the eastern continental slope and the southern slope of the Sokcho-Donghae Ridge reveal that these extensive debrites originated mainly from the west and north (Figs. 7 and 8A).

6. Discussion

Both the South Korea Plateau and the eastern continental slope of Korea show a distinctive zo-

nal distribution of mass-movement and gravity-flow deposits (Fig. 7): slides and slumps (type IV-1) on the upper to lower slopes of the ridges, seamount chains, and the eastern continental slope; debrites and turbidites (types II, III-2, IV-2, and IV-3) on the Onnuri Basin, troughs and the lower part of the eastern continental slope. The distinctive zonal distribution reflects that slope failures were initiated at the upper to lower slope of the ridges, seamount chains and the eastern continental slope and evolved successively into debris flows in the Onnuri Basin, troughs and the lower part of the eastern continental slope

(e.g., Chough et al., 1985a, 1997). In debris-flow deposits (types II and III-2), the gradual downslope decrease in size, spacing and relief of the surface forms suggest progressive dilution in flow concentration due to mixing of ambient water and removal of sediment by deposition during downslope movement (Lee et al., 1999). The turbidity currents evolved from debris flows would result in types IV-2 and IV-3 in the axis of troughs.

In the Onnuri Basin and troughs bounded upslope by large areas of slope failures (type IV-1), debris-flow deposits (types II and III-2) are dom-
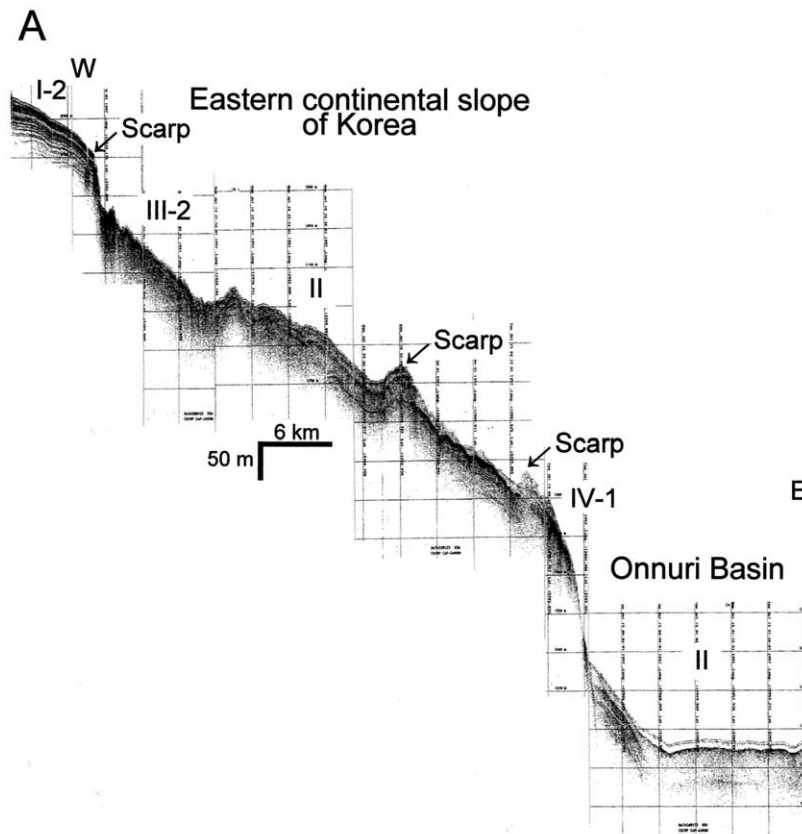

Fig. 8. Typical Chirp subbottom profiles showing occurrence and association of echo types according to the topographic provinces. For location of each profile, see Fig. 1B. (A) Eastern continental slope of Korea and Onnuri Basin in the South Korea Plateau. Type I-2 on the upper to middle continental slope changing downslope to types III-2 and II with the head scarp. At the lower continental slope, type II is dissected by scarps and remoulded into echo type IV-1. Note type II (debrites) draping over the entire floor of the Onnuri Basin. (B) Ridges and troughs in the South Korea Plateau. Extensive occurrence of type III-3 on broad, gently sloping areas of the ridges. Type III-3 is dissected by scarps at the upper slope of the ridges and transitional downslope to echo types IV-1 and III-2. (C) Seamount chains and troughs in the South Korea Plateau. Dominant occurrence of type IV-1 on the middle to lower slope of the seamount chains and types III-2 and IV-3 on the troughs.

inant (Fig. 7). On the other hand, the troughs surrounded by relatively small areas of slides and slumps (type IV-1) consist dominantly of turbidites with minor occurrence of debrites (types IV-2 and IV-3). These spatial distribution patterns suggest that the amounts of sediment involved in

sliding and slumping may have played an important role for controlling downslope evolution of sediment gravity flows. Where large amounts of sediment were involved in slope failures, debris flows evolving from slides and slumps tended to move further downslope and were transformed
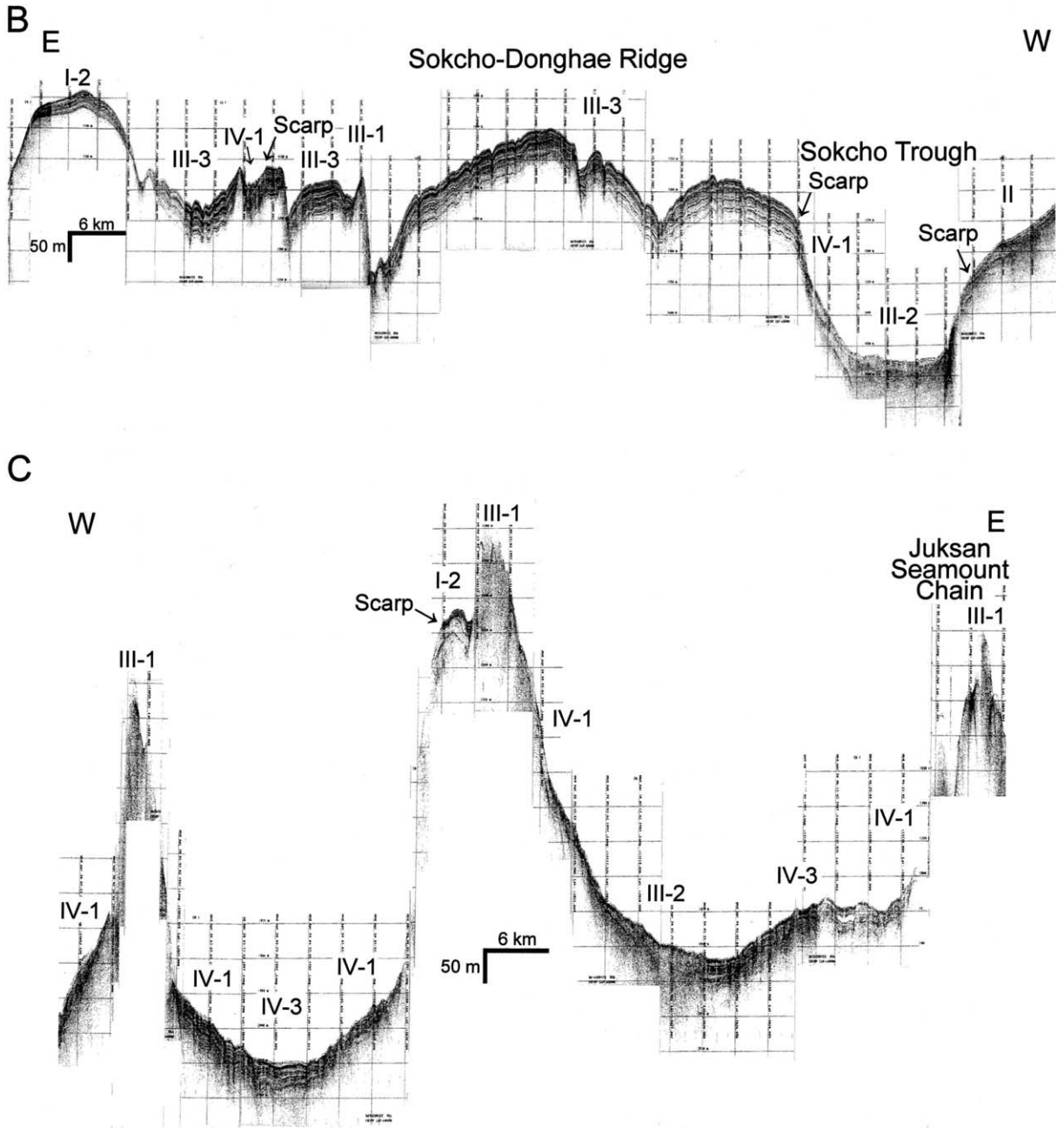

Fig. 8 (*Continued*).

into turbidity currents in the distal part. In contrast, slides and slumps of small amounts of sediments appear to have evolved into turbidity currents through debris flows within relatively short distances, forming abundant turbidites with minor debrites on the intervening troughs.

The South Korea Plateau and the eastern continental slope of Korea are subject to extensive creeps and slope failures with slides and slumps (Figs. 7 and 8). Mass movements generally occur when applied shear stresses reach above critical

shear strength of sediments (Prior and Coleman, 1984; Martinsen, 1994). In submarine environments, several causes such as high sedimentation rate, storm waves, earthquakes, biological processes and sea-level fall either increase applied shear stress or reduce critical shear strength of sediments, promoting mass movements (Maltman, 1994; Hampton et al., 1996; Stow et al., 1996). The South Korea Plateau and the eastern continental slope of Korea are characterized by low rates (ca. 5–7 cm/10^3 yrs) of sediment accu-

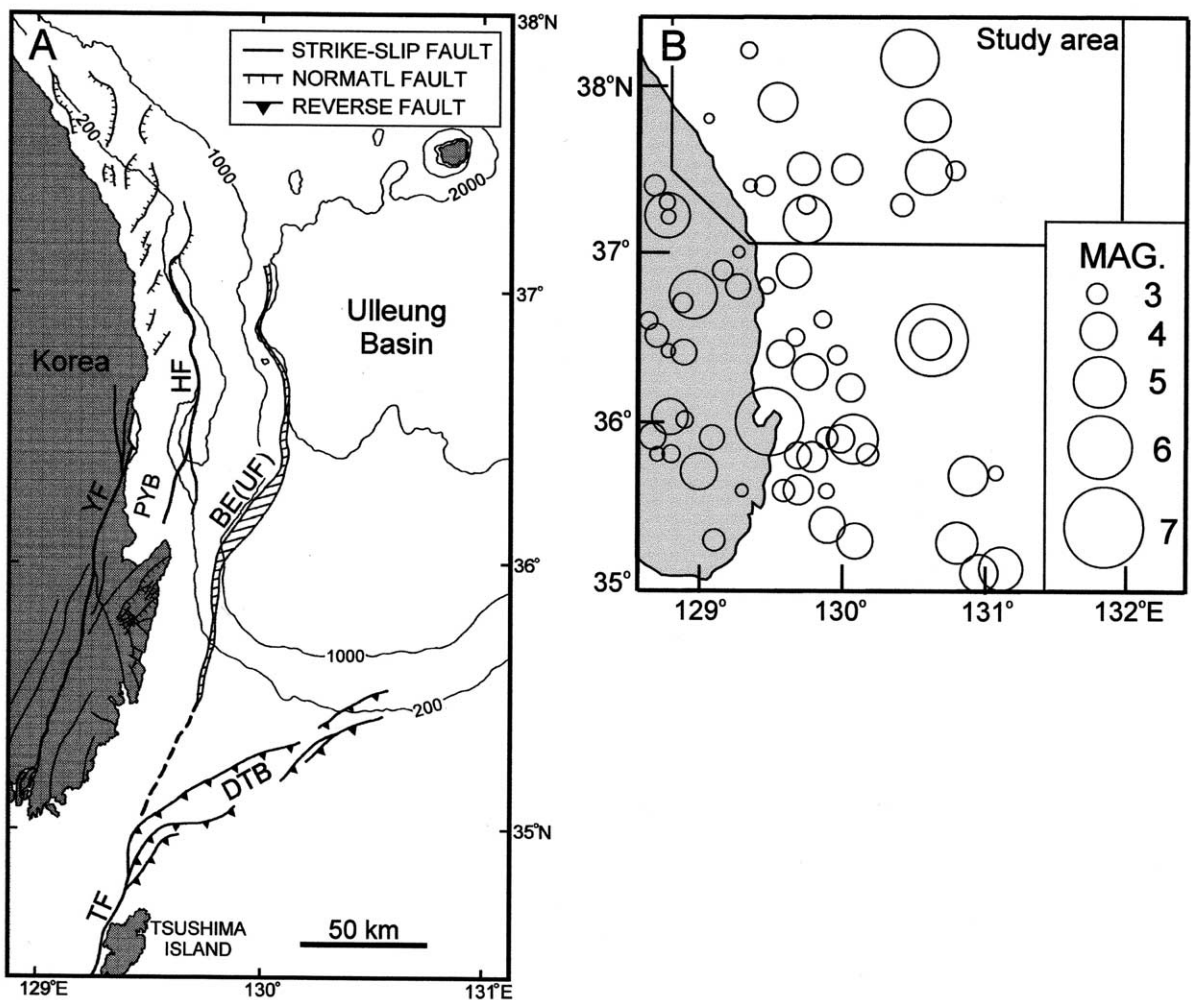Fig. 9. (A) Major geological structures of the eastern continental margin of Korea. DTB = Dolgorae Thrust Fault; HF = Hupo Fault; PYB = Pohang-Yongduk Basin; TF = Tsushima Fault; UF = Ulleung Fault; YF = Yangsan Fault. Modified from Chough et al. (2000). (B) Epicenters of earthquakes during 1905–1996 in the eastern continental margin of Korea and adjacent area. Modified from Baag et al. (1998).

mulation by receiving small amount of sediment via hemipelagic suspension settling (Yoon et al., 1996; Hong et al., 1997; KORDI, 1997), dismissing the possibility of generation of mass movements by static loading of sediments. The biologic processes are generally insufficient to cause large-scale slope instabilities in the South Korea Plateau and the eastern continental slope (e.g., Hecker, 1982; Hampton et al., 1996).

As voluminous slope failures and creeps on the South Korea Plateau and the eastern continental slope of Korea occur at water depths > 300 m, any destabilization of sediments covered by storm waves during lowering of sea level is unlikely. The eastern continental margin of Korea has been tectonically active with prominent N–S- to NNE–SSW-trending strike-slip (Ulleung Escarpment and Hupo Fault), normal and thrust faults that formed during the back-arc opening and closing of the Ulleung Basin (Yoon and Chough, 1995; Chough et al., 2000; Fig. 9A). Earthquakes have frequently occurred in the eastern Korean continental margin and its adjacent area (Baag et al., 1998; Fig. 9B), most likely triggering the deepwater (> 300-m-deep) creeps, slope failures and associated gravity flows.

The dominant bioturbated muds in type III-3 (creep deposits) associated upslope with type I-2 and the slightly displaced, intact blocks of type III-3 in slide and slump masses (type IV-1) suggest creep deformations and slope failures of type I-2 (pelagites/hemipelagites). These pelagites and hemipelagites are normally consolidated or slightly overconsolidated (KORDI, 1995; Yoon et al., 1996). These muddy sediments can be easily reduced in shear strength by earthquake loading (Maltman, 1994; Hampton et al., 1996). Accumulation of earthquake loading in undrained, muddy sediments is effective in reducing the critical shear strength of sediments to a sufficiently low level for failure to occur (Lee and Focht, 1976). Under these conditions, creeps and slope failures with slides and slumps can be triggered even by small earthquakes (Almagor and Wiseman, 1982).

In response to frequent earthquakes, pelagites/hemipelagites (type I-2) in the broad, gently sloping areas of the ridges were deformed by slow creep movements (type III-3), whereas type I-2

in the relatively steep slopes of the ridges, seamount chains and the eastern continental slope failed and formed slides and slumps (type IV-1) (Lee and Chough, 2001; Fig. 7). The abundant scarps in the slide and slump masses, and the remoulding of debrites into slide and slump masses are suggestive of several phases of slope failure generated by successive seismic events. Furthermore, the abundant crown cracks and small-scale extensional faults above the present head scarp and the step-like geometry of the failed masses show that the retrogressive sliding and slumping occurred concurrently in response to the successive earthquakes (Syvitski et al., 1987; Mulder and Cochonat, 1996; Gardner et al., 1999). Seismic shaking is generally effective in disturbing sediments in semi-enclosed topographic depressions by liquefaction (Syvitski et al., 1987; Mulder and Cochonat, 1996; Syvitski and Schafer, 1996), resulting in the deformation of turbidites and debrites (types IV-2 and IV-3) on the axis of the troughs.

7. Conclusions

A detailed analysis of high-resolution (Chirp) subbottom profiles from the South Korea Plateau and the eastern continental slope of Korea reveals a variety of mass-movement and gravity-flow deposits. Creeps and slope failures with slides and slumps (types III-3 and IV-1) occur extensively in the entire slope areas of ridges, seamount chains and the eastern continental slope. These voluminous mass movements, deeper than 300 m in water depth, were most likely generated by earthquakes that have frequently occurred in these areas. The mass-movement deposits change downslope to debrites (types II and III-2) and turbidites (types III-4, IV-2 and IV-3), suggesting successive downslope evolution from slide/slump to debris flows and turbidity currents. Debrites are dominant in the troughs and Onnuri Basin bounded by large areas of slides and slumps. In contrast, turbidites occur dominantly in the troughs bordered by small areas of slope failures. These distribution patterns imply that the amounts of sediment involved in sliding and

slumping have an important role for controlling downslope evolution of sediment gravity flows. Frequent seismic shakings would facilitate deformation of turbidites and debrites (types III-4, IV-2 and IV-3) in the axis of semi-enclosed troughs.

Acknowledgements

References

Almagor, G., Wiseman, G., 1982. Submarine slumping and mass movements on the continental slope of Israel. In: Saxov, S., Nieuwenhuis, J.K. (Eds.), Marine Slides and Other Mass Movements. Plenum Press, New York, pp. 95–128.

Baag, C.-E., Chang, S.-J., Jo, N.-D., Shin, J.-S., 1998. Evaluation of seismic hazard in southern part of Korea. In: Proceedings of 2nd International Symposium on Seismic Hazards and Ground Motion in the Region of Moderate Seismicity. Korea Earthquake Engineering Research Center and Earthquake Engineering Society of Korea, Seoul, pp. 31–50.

Chough, S.K., Jeong, K.S., Honza, E., 1985a. Zoned facies of mass-flow deposits in the Ulleung (Tsushima) Basin, East Sea (Sea of Japan). Mar. Geol. 65, 113–125.

Chough, S.K., Lee, H.J., Yoon, S.H., 2000. Marine Geology of Korean Seas, 2nd edn. Elsevier, Amsterdam, 313 pp.

Chough, S.K., Lee, S.H., Kim, J.W., Park, S.C., Yoo, D.G., Han, H.S., Yoon, S.H., Oh, S.B., Kim, Y.B., Back, G.G., 1997. Chirp (2–7 kHz) echo characters in the Ulleung Basin. Geosci. J. 1, 143–153.

Chough, S.K., Mosher, D.C., Srivastava, S.P., 1985b. Ocean Drilling Program (ODP) site survey (Hudson 84-30) in the Labrador Sea: 3.5 kHz profiles. Geol. Surv. Can. Paper 85-1B, 33–41.

Damuth, J.E., 1975. Echo characters of the western equatorial Atlantic floor and its relationship to the dispersal and distribution of terrigenous sediments. Mar. Geol. 18, 17–45.

Damuth, J.E., 1980. Use of high-frequency (3.5–12 kHz) echograms in the study of near-bottom sedimentation processes in the deep-sea: a review. Mar. Geol. 38, 51–75.

Damuth, J.E., Embley, R.W., 1981. Mass-transport processes on Amazon Cone: western equatorial Atlantic. Am. Assoc. Pet. Geol. Bull. 65, 629–643.

Damuth, J.E., Hayes, D.E., 1977. Echo character of the east Brazilian continental margin and its relationship to sedimentary processes. Mar. Geol. 24, 73–95.

Dowdeswell, J.A., Kenyon, N.H., Laberg, J.S., 1997. The glacier-influenced Scoresby Sund Fan, East Greenland continental margin: evidence from GLORIA and 3.5 kHz records. Mar. Geol. 143, 207–221.

Embley, R.W., 1976. New evidence for ocurrence of debris flow deposits in the deep sea. Geology 4, 371–374.

Embley, R.W., Jacobi, R.D., 1977. Distribution and morphology of large submarine sediment slides and slumps on Atlantic continental margins. Mar. Geotechnol. 2, 205–228.

Flood, R.D., 1980. Deep-sea sedimentary morphology: modelling and interpretation of echo-sounding profiles. Mar. Geol. 38, 77–92.

Gardner, J.V., Prior, D.B., Field, M.E., 1999. Humbolt Slide – a large shear-dominated retrogressive slope failure. Mar. Geol. 154, 323–338.

Hampton, M.A., Lee, H.J., Locat, J., 1996. Submarine landslides. Rev. Geophys. 34, 33–59.

Hecker, B., 1982. Possible benthic fauna and slope instability relationships. In: Saxov, S., Nieuwenhuis, J.K. (Eds.), Marine Slides and Other Mass Movements. Plenum Press, New York, pp. 335–348.

Hill, P.R., Moran, K.M., Blasco, S.M., 1982. Creep deformation of slope sediments in the Canadian Beaufort Sea. Geo-Mar. Lett. 2, 163–170.

Hollister, C.D., Heezen, B.C., 1972. Geologic effects of ocean bottom currents: western North Atlantic. In: Gordon, A.L. (Ed.), Studies in Physical Oceanography. Gordon and Breach, London, pp. 37–66.

Hong, G.H., Kim, S.H., Chung, C.S., Kang, D.J., Shin, D.H., Lee, H.J., Han, S.J., 1997. ^{210}Pb-derived sediment accumulation rates in the southwestern East Sea (Sea of Japan). Geo-Mar. Lett. 17, 126–132.

Jacobi, R.D., Hayes, D.E., 1982. Bathymetry, microphysiography and reflectivity characteristics of the west African margin between Sierra Leone and Mauritania. In: von Rad, U., Hinz, K., Sarnthein, M., Seibod, E. (Eds.), Geology of the Northwest African Continental Margin. Springer-Verlag, Berlin, pp. 182–212.

Jacobi, R.D., Hayes, D.E., 1992. Northwest African continental rise: effects of near-bottom processes inferred from high-resolution seismic data. In: Poag, C.W., de Graciansky, P.C. (Eds.), Geologic Evolution of Atlantic Continental Rises. Reinhold, New York, pp. 293–326.

Klaus, A., Ledbetter, M.T., 1988. Deep-sea sedimentary processes in the Argentine Basin revealed by high-resolution seismic records (3.5 kHz echograms). Deep-Sea Res. 35, 899–917.

KORDI (Korea Ocean and Research Development Institute),

1995. Basin Structures and Past Changes in the East Sea, Korea (BASAPES-95). 407 pp. (in Korean with English abstract).

KORDI (Korea Ocean and Research Development Institute), 1997. Marine Environment Changes and Basin Evolution in the East Sea, Korea (MECBES-97). 657 pp. (in Korean with English abstract).

Laine, E.P., Damuth, J.E., Jacobi, R., 1986. Surficial sedimentary processes revealed by echo-characters mapping in the western North Atlantic Ocean. In: Vogt, P.R., Tucholke, B.E. (Eds.), The Western North Atlantic Region. Geology of North America, M, pp. 427–436.

LeBlanc, L.R., Panda, S., Schock, S.G., 1992. Sonar attenuation modeling for classification of marine sediments. J. Acoust. Soc. Am. 91, 116–126.

Lee, K.L., Focht, J.A., 1976. Strength of clay subjected to cyclic loading. Mar. Geotechnol. 1, 165–168.

Lee, S.H., Chough, S.K., 2001. High-resolution (2–7 kHz) acoustic and geometric characters of submarine creep deposits in the Korea Plateau, East Sea. Sedimentology 48, 629–644.

Lee, S.H., Chough, S.K., Back, G.G., Kim, Y.B., Sung, B.S., 1999. Gradual downslope change in high-resolution acoustic characters and geometry of large-scale submarine debris lobes in Ulleung Basin, East Sea (Sea of Japan), Korea. Geo-Mar. Lett. 19, 254–261.

Maltman, A., 1994. Introduction and overview. In: Maltman, A. (Ed.), The Geological Deformation of Sediments. Chapman and Hall, London, pp. 1–35.

Martinsen, O., 1994. Mass movements. In: Maltman, A. (Ed.), The Geological Deformation of Sediments. Chapman and Hall, London, pp. 127–165.

Masson, D.G., Canals, M., Alonso, B., Urgele, R., Huhnerbach, V., 1998. The Canary debris flow: source area morphology and failure mechanisms. Sedimentology 45, 411–432.

Middleton, G.V., Hampton, M.A., 1973. Mechanics of flow and deposition. In: Bouma, A.H. (Ed.), Turbidites and Deep Water Sedimentation. Soc. Econ. Paleo. Miner. Pacific Section, Short Course, pp. 1–38.

Mulder, T., Cochonat, P., 1996. Classification of offshore mass movements. J. Sediment. Res. 66, 43–57.

Nardin, T.R., Hein, F.J., Gorsline, D.S., Dewards, B.D., 1979. A review of mass movement processes, sediment and acoustic characteristics in slope and base-of-slope systems versus canyon-fan-basin floor systems. In: Doyle, L.J., Pilkey, O.H. (Eds.), Geology of Continental Slopes. Soc. Econ. Paleo. Miner. Spec. Publ. 27, 61–73.

Normark, W.R., Gutmacher, C.E., 1988. Sur submarine slide, Monterey Fan, central California. Sedimentology 35, 629–647.

O'Leary, D.W., Laine, E., 1996. Proposed criteria for recognition of intrastratal deformation features in marine high-resolution seismic reflection profiles. Geo-Mar. Lett. 16, 305–312.

Piper, D.J.W., Cochonat, P., Morrison, M.L., 1999. The sequence of events around the epicentre of the 1929 Grand Banks earthquake: initiation of debris flows and turbidity current inferred from sidescan sonar. Sedimentology 46, 79–97.

Piper, D.J.W., Farre, J.A., Shor, A., 1985. Late Quaternary slumps and debris flows on the Scotian slope. Geol. Soc. Am. Bull. 96, 1508–1517.

Pratson, L.F., Laine, E.P., 1989. The relative importance of gravity-induced versus current-controlled sedimentation during the Quaternary along the mideast United-States outer continental-margin revealed by 3.5 kHz echo character. Mar. Geol. 89, 87–126.

Prior, D.B., Coleman, J.M., 1984. Submarine slope instability. In: Brunsden, D., Prior, D.B. (Eds.), Slope Instability. John Wiley and Sons, New York, pp. 419–455.

Schock, S.G., LeBlanc, L.R., Mayer, L.A., 1989. Chirp sub-bottom profiler for quantitative sediment analysis. Geophysics 54, 445–450.

Stow, D.A.V., Reading, H.G., Collison, J.D., 1996. Deep seas. In: Reading, H.G. (Ed.), Sedimentary Environments: Processes, Facies and Stratigraphy. Blackwell Science, Oxford, pp. 395–453.

Syvitski, J.P.M., Schafer, C.T., 1996. Evidence for an earthquake-triggered basin collapse in Saguenay Fjord Canada. Sediment. Geol. 104, 127–153.

Syvitski, J.P.M., Burrell, D.C., Skei, J.M., 1987. Fjords: Processes and Products. Springer-Verlag, New York, 379 pp.

Wynn, R.B., Masson, D.G., Stow, D.A.V., Weaver, P.P.E., 2000. The Northwest African slope apron: a modern analogue for deep-water system with complex seafloor topography. Mar. Petrol. Geol. 17, 253–265.

Yoon, S.H., Chough, S.K., 1995. Regional strike slip in the eastern continental margin of Korea and its tectonic implications for the evolution of Ulleung Basin, East Sea (Sea of Japan). Geol. Soc. Am. Bull. 107, 83–97.

Yoon, S.H., Lee, H.J., Han, S.J., Kim, S.R., 1996. Quaternary sedimentary processes on the east Korean continentaly slope. J. Geol. Soc. Korea 32, 250–266 (in Korean with English abstract).

Zaragosi, S., Auffret, G.A., Faugères, J.-C., Garlan, T., Pujol, C., Cortijo, E., 2000. Physiography and recent sediment distribution of the Celtic Deep-sea Fan, Bay of Biscay. Mar. Geol. 169, 207–237.